ACS APPLIED MATERIALS & INTERFACES

Research Article

www.acsami.org

Multiresponsive Hydrogel Coassembled from Phenylalanine and Azobenzene Derivatives as 3D Scaffolds for Photoguiding Cell Adhesion and Release

Guo-Feng Liu, Wei Ji, Wan-Lin Wang, and Chuan-Liang Feng*

State Key Lab of Metal Matrix Composites, School of Materials Science and Engineering, Shanghai Jiaotong University, 800 Dongchuan Road, Shanghai 200240, China

Supporting Information

ABSTRACT: A multiresponsive hydrogel system coassembled from phenylalanine derivative gelator (LPF2) and azobenzene (Azo) derivative (PPI) is constructed, which can respond to temperature, pH, host−guest interaction, and photoirradiation. A set of techniques including circular dichroism, Fourier transform infrared spectroscopy, ^{1}H NMR, and X-ray powder diffraction confirm that the hydrogel is formed through hydrogen bonds between amide moieties/pyridine and carbonyl groups, enduing the coassembled hydrogel with multiresponsive properties that make it possible to control cell encapsulation and release in three-dimensional environments under multistimulus, for example, UV irradiation. This study brings a novel approach to develop multistimuli-responsive hydrogels by coassembly of various responsive components for biomedical interest, for example, the controlled delivery of various therapeutic biological agents.

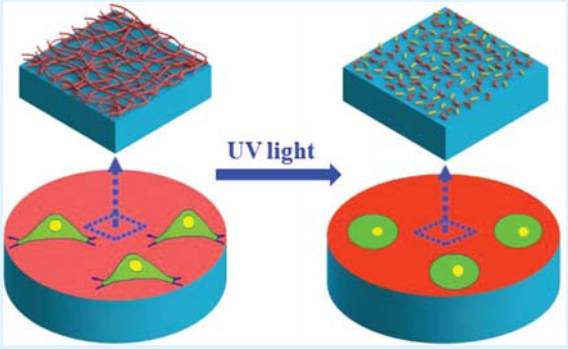

KEYWORDS: *multiresponsive, supramolecular hydrogel, coassembly, cell release, three-dimensional*

INTRODUCTION

Manipulating the inherent cell adhesion response to external stimuli for simulating the complex function of living systems in vitro is of high interest both in medical basic research and for biotechnological applications.[1,2] This motivation has led to the development of new biocompatible approaches to tailor cellular microenvironments.[3−5] However, with few exceptions, the existing technologies are mostly used to control cell adhesion on two-dimensional (2D) surfaces.[6−10] It still remains a big challenge to regulate cell adhesion in three-dimensional (3D) environments, especially, to develop smart 3D scaffolds for resembling the living systems as a response to the applied stimuli.[11−15]

Supramolecular hydrogels have been extensively studied as smart 3D scaffolds due to their excellent abilities to simulate the natural extracellular matrix (ECM) and respond to various external stimuli, such as temperature,[15] redox reagents,[16] ultrasound,[17] and light irradiation.[4,18] Among various available stimuli, light is particularly attractive as its intensity and wavelength can be easily tuned, which allows the remote activation of materials with relatively high spatial and temporal precision. Thus, photoresponsive hydrogels are potential 3D scaffolds to spatially and temporally control the microenvironments of encapsulated cells through a precision "on−off" switch.[4]

Recently, a growing number of multistimuli-responsive organogels have been designed.[19−23] However, it is still difficult to design simple and effective hydrogelator having multi-responsive abilities.[16] Alternatively, this drawback may be avoided by simply employing various responsive molecules to form multicomponent hydrogels through controllable coassembly.[24] In this paper, a multiresponsive hydrogel system coassembled from phenylalanine derivative gelator (LPF2) and azobenzene (Azo) derivative (PPI) is constructed, which is driven by hydrogen bonds between amide moieties/pyridine and carbonyl groups (Scheme 1). First, the incorporation of the Azo group makes it possible for the hydrogel to be light-responsive, leading to sequential effect on the intermolecular hydrogen bonding interactions between LPF2 and PPI. In addition, the Azo group can also induce host−guest interactions with the α-cyclodextrin (α-CD) molecule. Finally, phenylalanine groups from LPF2 provide the possibility to tune the self-assembly by adjusting pH and further enhance gelation ability.[25] To explore the feasibility of the multistimuli responsive hydrogels for regulating cell behaviors in 3D environments, the photoguiding cell adhesion and release is investigated in detail.

Received: September 10, 2014
Accepted: November 5, 2014
Published: November 5, 2014

ACS Publications © 2014 American Chemical Society

Scheme 1[a]

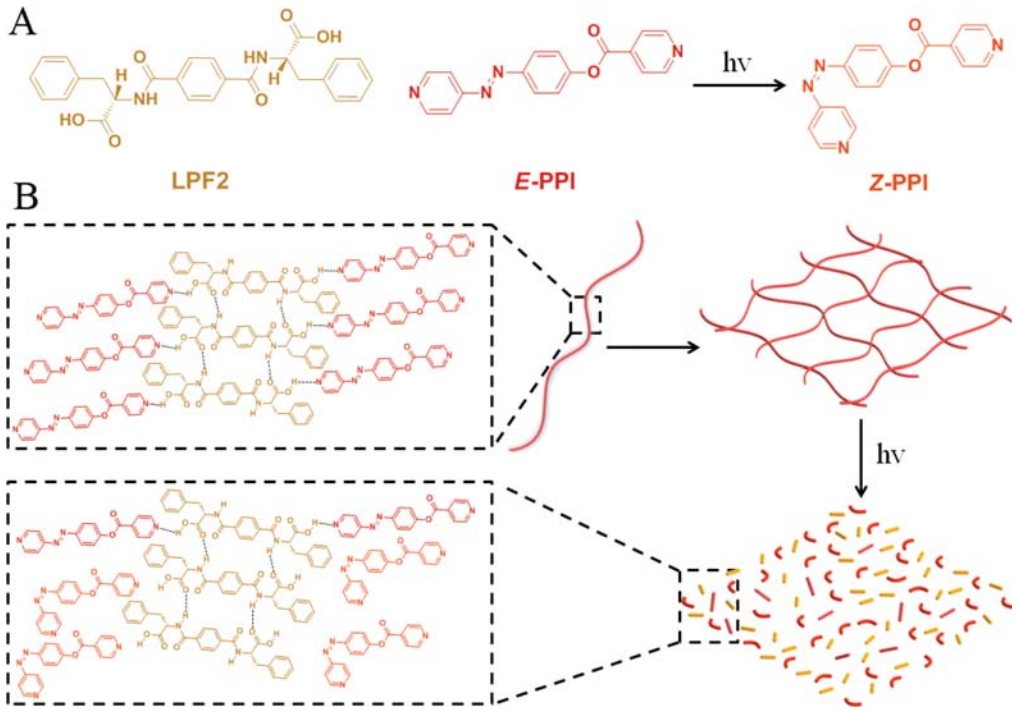

[a](A) Chemical structures of the gelator LPF2 and azobenzene derivative PPI (*E*-PPI represents trans isomer and *Z*-PPI represents cis isomer). (B) Schematic demonstration of co-assembly and disassembly of two-component hydrogel LPF2-PPI networks. Black dotted line represents hydrogen bonds between amide moieties/pyridine and carbonyl groups; the yellow rod represents LPF2; the red rod stand for *E*-PPI; the orange crook represents *Z*-PPI.

EXPERIMENTAL SECTION

Materials. All chemicals were purchased from Aldrich and used without further purification. Phenylalanine derivative gelator (LPF2) and azobenzene derivative (PPI) were synthesized with high yield through conventional liquid-phase reaction according to Supporting Information, Scheme S1. The synthesis method is described in the Supporting Information. NMR experiments were performed by using Bruker Advance III 400 Instrument operated at 400 MHz. Fast atom bombardment mass spectrometry (FAB-MS) spectra were obtained by a JEOL JMS 700 mass spectrometer.

Gelation. The LPF2-PPI hydrogel with 0.2 wt % LPF2-PPI is used as an example to describe the preparation procedure. LPF2-PPI (2 mg/mL, 1:1 mixture of LPF2 and PPI) was suspended in a septum-capped 5 mL glass vial and heated (~100 °C) until the solid was dissolved, after which the solution was allowed to cool to room temperature. Hydrogel was considered to have formed when no gravitational flow occurred upon inversion of the vial.

Freeze-Drying. Both LPF2 and LPF2-PPI hydrogels were kept in liquid nitrogen for 30 min, then transferred to the lyophilizer, and kept there until all the frozen water in the hydrogels was sublimated in vacuum.

Scanning Electronic Microscopy. Scanning electronic microscopy (SEM) measurements were carried out using an FEI QUANTA 250 Microscope. Samples were prepared by depositing dilute solutions of gel on silicon slice, drying them under vacuum, and coating them with gold on a sputtering coater.

Transmission Electron Microscopy. Transmission electron microscopy (TEM) from Tecnai G2 Spirit Biotwin (FEI, U.S.) was used to characterize the nanofibrous xerogels. The LPF2 and LPF2-PPI samples for TEM observation were prepared by placing drops of the diluted LPF2 and LPF2-PPI aqueous suspension onto copper grids, which were then dried under ambient conditions prior to being introduced into the TEM chamber (JEM-2010).

Circular Dichroism Spectroscopy. Circular dichroism (CD) spectra were collected on a JASCO J-815 CD spectrometer with bandwidth of 1.0 nm. CD spectra of hydrogels were recorded in the UV region (190−400 nm) using a 0.1 mm quartz cuvette with the total gelators concentration at 0.2 wt %.

Rheological Measurements. The rheological properties of hydrogels were measured using a rheometer (Gemini HRnano). The measurements were performed using a dynamic frequency sweep test with 1% strain over a range of frequencies (0.01−10 Hz) at 25 °C.

Fourier Transform Infrared Spectroscopy. Fourier transform infrared (FT-IR) spectra of xerogels were taken using a Bruck EQUINOX55 Instrument. The KBr disk technique was used for the solid-state measurement. The samples were scanned between the wavelengths of 4000 and 400 cm^{-1} at an interval of 1.9285 cm^{-1}.

X-ray Powder Diffraction. The X-ray powder diffraction (XRD) patterns were obtained from xerogels. The LPF2 and LPF2-PPI hydrogels were filtered and dried upon vacuum to get xerogel. The XRD pattern was recorded on a D8 Advance instrument from Bruker AXS Company (step size: 0.02° step time: 0.8 s).

2D Cell Culture. Hydrogels were statically seeded with mouse embryonic fibroblast (NIH 3T3) cell (cell bank of the Chinese Academy of Sciences). Cells were maintained in Dulbecco's Modified Eagle Medium (DMEM), supplemented with 10% fetal calf serum. All cells were cultured in a 37 °C and 5% CO_2 incubator.

3D Cell Culture. To encapsulate cells, cell solution was mixed into concentrated LPF2-PPI and LPF2 dimethyl sulfoxide (DMSO) solution at 37 °C, and the final DMSO concentration for the mixtures was 3.3%. One milliliter of cell-gel constructs (2×10^6 cells per mL) was then transferred to a 24-well culture plate in triplicate. After 30 min, an extra 2 mL of complete medium (DMEM containing calf serum) was applied on top of each cell-gel construct, and the plate was maintained in a 37 °C and 5% CO_2 incubator. The medium on top of the constructs was changed after 2 h of culture and then daily. Finally

the encapsulated cells were analyzed and quantified by using CCK-8 assay at a series of time points (4 h, 1 d, 3 d, 5 d, and 7 d).

CCK-8 Assay. The toxicity of LPF2-PPI hydrogel to cells was investigated by CCK-8 assay. NIH 3T3 cells were plated at a density of 1×10^4 cells per well in complete medium in 24-well cell culture plates and grown for 24 h. The cells were then exposed to a series of concentrations of LPF2-PPI composite for 24 h, and the viability of the cells was measured using the CCK-8 method. The supernatant of each well was discarded, followed by the additional 50 μL of phosphate-buffered saline (PBS) used to washed each well three times, and then replaced with CCK-8 solution, and the cells were further incubated for an additional 2 h at 37 °C. Finally, the optical density (OD) was read at a wavelength of 450 nm by ELIASA. Relative cell viability was expressed as % = ([OD] test/[OD]control) × 100.

Live−Dead Staining Assay. The viability of the cells was assessed with a fluorescent live−dead staining assay (Dojindo Corp.). The medium was removed, and the constructs were washed twice with PBS. Then 200 μL of the PBS assay solution containing 2 μM calcein AM (3',6'-Di(O-acetyl)-4',5'-bis[N,N-bis(carboxymethyl)-aminomethyl]fluorescein, tetraacetoxymethyl ester) and 4 μM propidium iodide (PI) was pipetted onto each cell-gel construct. After 15 min of incubation under humidified atmosphere of 5% CO_2 at 37 °C, removing the staining solution, and washing with PBS three times, the labeled cells were then viewed under an inverted fluorescence microscope with excitation filters of 494 and 545 nm. Quantitative number of live/dead cells on hydrogels was determined by using the program ImageJ form the National Institute of Health, U.S.

RESULTS AND DISCUSSION

LPF2 and PPI were synthesized based on the procedure in Supporting Information, Scheme S1. Compared with the transparent unstable LPF2 hydrogel (Supporting Information, Figures S1a and S2), the homogeneous orange composite hydrogel of LPF2-PPI (1:1 mixture of LPF2 and PPI) maintained longer as no-flowing hydrogel (Supporting Information, Figure S1b) and exhibited multiresponsive property (Figure 1). The thermoresponsive property of the

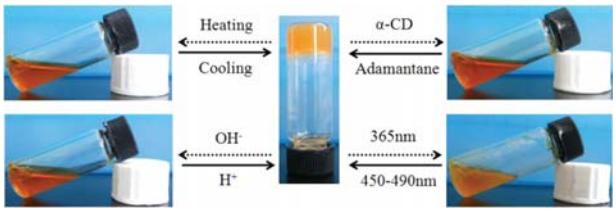

Figure 1. Photographs of the reversible gel−sol transition of LPF2-PPI hydrogel triggered by multiple stimuli (temperature, pH, host−guest interaction, and photoirradiation, respectively).

LPF2-PPI hydrogel was directly confirmed by the dissolution with increasing temperature and gelation upon cooling (Figure 1). Because of the pH-sensitive property of the phenylalanine group in LPF2 and the pyridine group in PPI, the LPF2-PPI hydrogel can also be dissolved in basic solution and reformed in acidic and neutral environment (Figure 1). The operational pH range for LPF2-PPI hydrogel formation is from 1 to 10, and a liquid state can be obtained once the pH of solution is above 10 (Supporting Information, Figure S3).

Because of well-known host−guest interactions between α-CD and Azo compound,[26] the reversible gel−sol transitions can also be achieved (Figure 1) by adjusting the host−guest interactions. Scanning electron microscopy (SEM) images showed that there was no nanofiber formation after adding α-CD into LPF2-PPI gel (Supporting Information, Figure S4a). The macroscopic gel could be recovered by adding adamantane into the sol with the similar fibrillar morphology (Supporting Information, Figure S4b), which was ascribed to much stronger interactions between α-CD and adamantane than those between α-CD and Azo units.[26] It indicated that macroscopic gel assembly could be highly regulated by host−guest interactions between the Azo and α-CD molecules.

As the photoisomerization property of the Azo units, the gel−sol phase transitions could be further triggered by UV and visible light. Upon UV (365 nm) irradiation, the stable orange gels were found to collapse gradually until a transparent solution was formed. Microscopic images of the LPF2-PPI xerogels (Figure 2A,B) confirmed that the hydrogels were

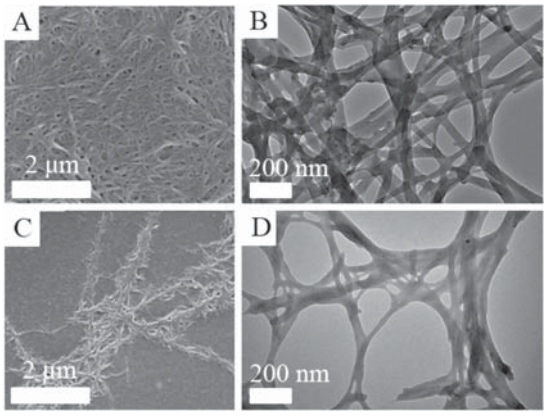

Figure 2. SEM images of LPF2-PPI gel before (A) and after (C) UV irradiation (365 nm) for 30 min. TEM images of LPF2-PPI gel before (B) and after (D) UV exposure for 30 min.

composed of the well-organized fibrils having widths of 30−60 nm and maximium lengths of 1 mm. Typically, an entangled fibrous network was observed for the gels before UV irradiation (Figure 2A,B), while the broken fibers and corresponding degradation of fibrous network were observed after UV irradiation for 30 min (Figure 2C,D). The reversible formation of the hydrogel with entangled fibrous networks was achieved again by the subsequent visible light irradiation (Figure 1 and Supporting Information, Figure S4c).

To further study the phototriggered gel−sol phase transitions of the hydrogels, the configurable changes of Azo chromophores were investigated by simultaneous UV−vis and CD spectra. A gradual decrease of the CD intensity at 266 nm (characteristic of the CO-NH) was observed until it disappeared after UV irradiation for 60 min because of the photoisomerization of the Azo groups (Figure 3). CD spectra of the gel suggested a continuous decrease in the α-helix secondary structure with increasing UV exposure time. Interestingly, the reversible increased CD signal was achieved again by the subsequent visible light irradiation (Supporting Information, Figure S5). In comparison, CD spectra of the LPF2 gel did not show any changes after UV exposure for 60 min (Supporting Information, Figure S6).

The rheological properties of the LPF2-PPI hydrogels were further investigated by using rheometer. Dynamic frequency sweep showed that G' of the gels was at the kilopascal level (ca. 5000 Pa, Figure 4), comparable to those of polymeric hydrogel used for 3D cell encapsulation.[27] Compared to LPF2 gel (Supporting Information, Figure S7), the G' of LPF2-PPI gel

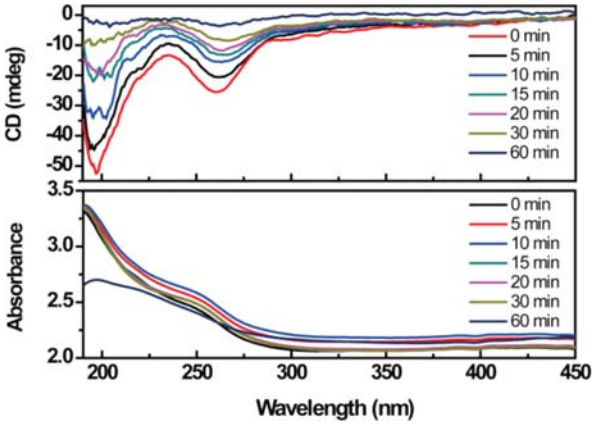

Figure 3. CD and UV−visible absorption spectra of LPF2-PPI hydrogel under UV irradiation (365 nm) for different times.

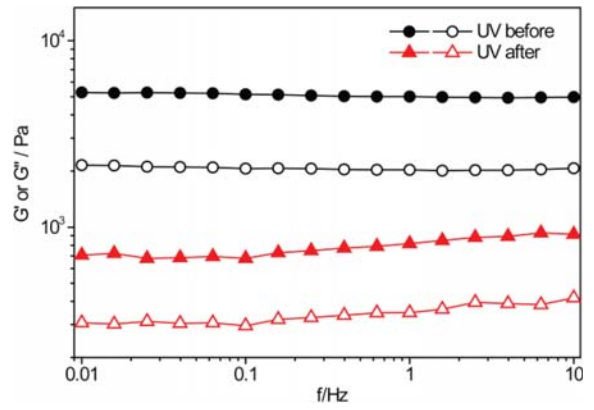

Figure 4. Dynamic frequency sweep of LPF2-PPI hydrogel before (black) and after (red) UV irradiation for 30 min. (total gelator concentration = 0.20 wt %). Solid black circles (●) and solid red triangles (▲) represent elastic modulus G'; hollow black circles (○) and hollow red triangles (△) stand for viscous modulus G''.

exhibited stability in the frequency range of 0.01−10 rad/s, demonstrating that LPF2-PPI gel has better mechanical stability but with similar stiffness (the elastic modulus of both hydrogels was ca. 5000 Pa). Upon UV irradiation for 30 min, both G' and G'' of the dissociated LPF2-PPI gel system became much lower than the intact one and showed some frequency dependence (Figure 4). The results clearly suggested that the stable LPF2-PPI gel was attributed to the coassembly of LPF2 and PPI.

To explore the mechanism of the coassembly for LPF2-PPI gel, the gels and corresponding solid powders were first studied by FT-IR spectroscopy (Figure 5 and Supporting Information, Table S1). The LPF2-PPI gel clearly exhibited new strong bands at 1637 and 1542 cm^{-1}, corresponding to the characteristic amide I and amide II bands at 1629 and 1552 cm^{-1} of the LPF2 molecule, whereas the peak at 1724 cm^{-1}, assigned to the carboxyl group of LPF2, corresponds to the characteristic peak at 1740 cm^{-1}.[28] Furthermore, the resulting LPF2-PPI gel clearly exhibited new strong bands at 3439 and 3328 cm^{-1} due to the hydrogen bond formations between amide moieties/pyridine and carboxyl group.[29]

The contribution of intermolecular hydrogen bonds to the gelation was further evaluated by ^1H NMR (Supporting Information, Figure S9). Broad NMR signals for the aromatic

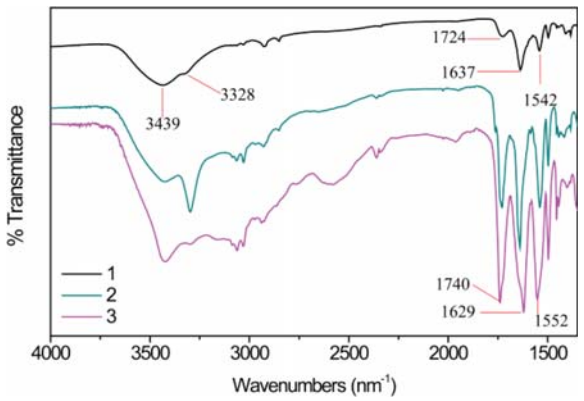

Figure 5. FTIR curves of (1) LPF2-PPI xerogel, (2) PPI powder, and (3) LPF2 powder.

hydrogen atoms indicated extensive aggregation (Supporting Information, Figure S9, middle) for LPF2-PPI gels (D_2O/DMSO, 2:1). Because of the strong electron-absorbing effect of the carboxyl groups in LPF2 structure, the sharp signals of the heteroaromatic protons in PPI were steadily broadened and shifted downfield (e.g., the proton of the pyridine ring is shifted from 8.60 to 8.94 ppm). In addition, a prominent reflection characteristic of a typical $\pi-\pi$ stacking distance was not observed in the wide-angle region at 3.5 Å (2θ = 25.4°) of the XRD patterns (Supporting Information, Figure S10), which suggested that there was no $\pi-\pi$ stacking in the coassembly of LPF2-PPI.[30] These experiments clearly demonstrated that the coassembly LPF2-PPI gel was attributed to intermolecular hydrogen bonding interactions between amide moieties/pyridine and carboxyl group.

To demonstrate the possible applications of LPF2-PPI gels as multistimuli scaffolds for regulating cell encapsulation and release in 3D, mouse embryonic fibroblast cell line (NIH 3T3) was selected as the model cells. The LPF2-PPI hydrogel exhibited negligible toxicity as shown in the test of CCK-8 assay (Supporting Information, Figures S11 and S12). First, the cell adhesion and detachment on the hydrogel films were evaluated. The freeze-dried LPF2 and LPF2-PPI gel films were immersed in cell culture medium containing 1.0×10^4 NIH 3T3 cells. After 24 h, the fibroblasts could adhere efficiently and spread well on all types of substrates (Figure 6a and Supporting Information, Figure S13a), indicating that both hydrogels were bioadherent. When the cultivation medium was exposed to UV irradiation for 30 min, a rapid cell rounding was observed on the LPF2-PPI gel films (Figure 6b), allowing their facile detachment and harvesting by gently rinsing at room temperature (Figure 6c). The recovered cells adhered well and kept good viability after reseeding on the poly(styrene) (PS) plate and 6 h of incubation (Figure 6d−f). The amount of recovered cell was 92.76% of that adhered on LPF2-PPI film before UV irradiation, with only few residual cells adhered on film after UV irradiation and rinse (Figure 6g). Interestingly, 97.25% of the recovered cells still keep alive, and just few cells were dead (Figure 6h), which suggested that cell viability was not affected by UV irradiation. However, the cells cultured on the LPF2 hydrogel film displayed a negligible change after UV light irradiation and rinse (Supporting Information, Figure S13b,c). Thus, the cell adhesion and detachment mechanism of cell was further illustrated by means of spectra in Figure 3B. NIH 3T3 cells adhered efficiently and spread well on intact

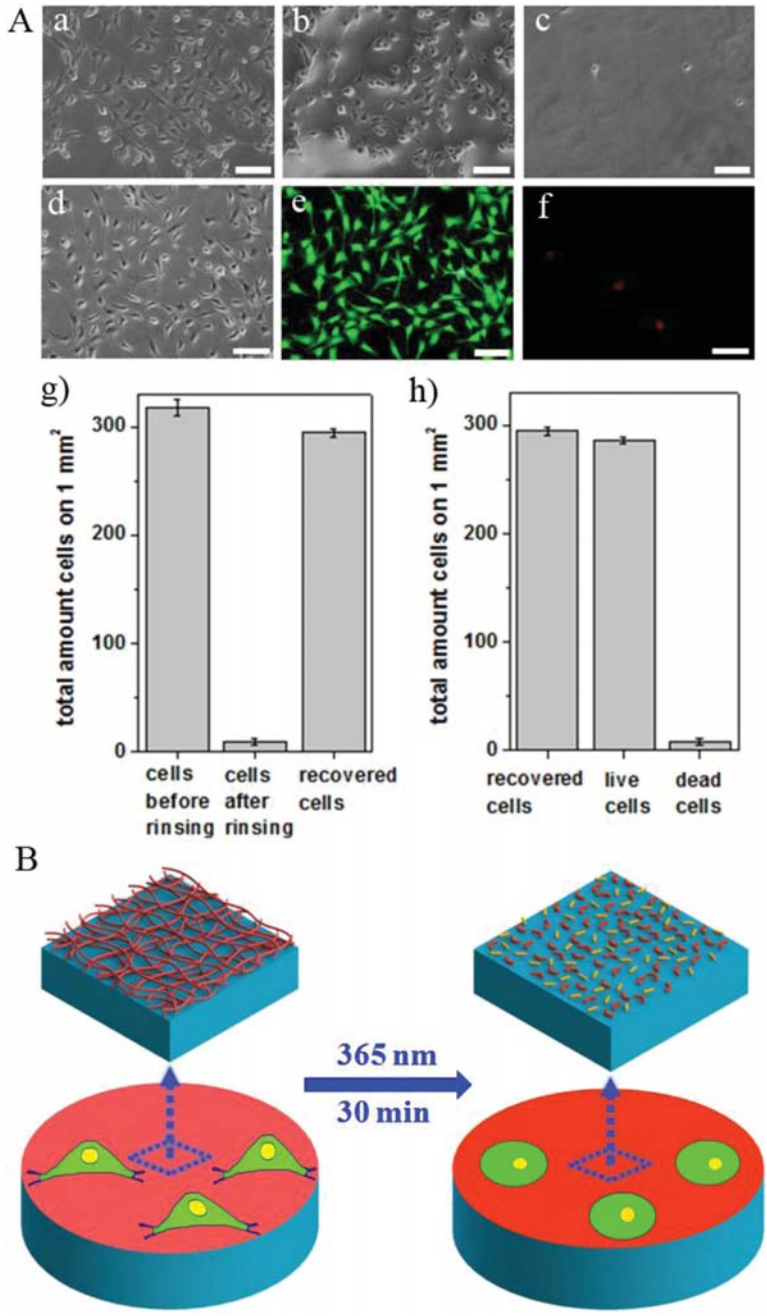

Figure 6. (A) (a) The bright field images of NIH 3T3 cells on LPF2-PPI hydrogel film after 24 h of incubation and (b) the corresponding images of (a) after UV irradiation for 30 min. (c) The bright field images of cells adhered on LPF2-PPI film after UV irradiation and gentle rinsing at room temperature. The viability of the recovered cells harvested from gentle rinsing were reseeded on PS plate and illustrated with bright field image (d) and the corresponding live/dead assay (e, f), respectively. (g) Density of cells adhered on film before rinsing, after rinsing, and the harvested cell reseeded on PS plate was determined to be 318, 9, and 295 mm^{-2}, respectively. (h) Density of the reseeded cells illustrated with total, live, and dead cells was 295, 286, and 8 mm^{-2}, respectively. The cells were quantified by using the program ImageJ. Scale bar = 100 μm. (B) The panels show a schematic view of the gel fiber coatings and NIH 3T3 cells adhered on the films before (left) and after (right) UV irradiation. The yellow rod represents LPF2, and the orange crook is *Z*-PPI.

fibers of LPF2-PPI gel film before UV irradiation (left). After UV irradiation for 30 min, the intermolecular hydrogen bonding interactions between LPF2 and PPI were damaged due to the photoisomerization of Azo groups, leading to broken fibers and the appearance of round cells (right). It means that the LPF2-PPI films can be switched from cell-attractive to cell-repellent under UV irradiation.

The possibly manipulating cell encapsulation and release in 3D was then carried out in LPF2-PPI gels. The cryo-dried xerogel investigated by SEM showed the 3D entangled nanofibrous network and the highly interconnected pores with the average diameter of tens of micrometers (Supporting Information, Figure S14), ensuring the compatible scale for cell encapsulating in 3D environment.[31,32] NIH 3T3 cells were

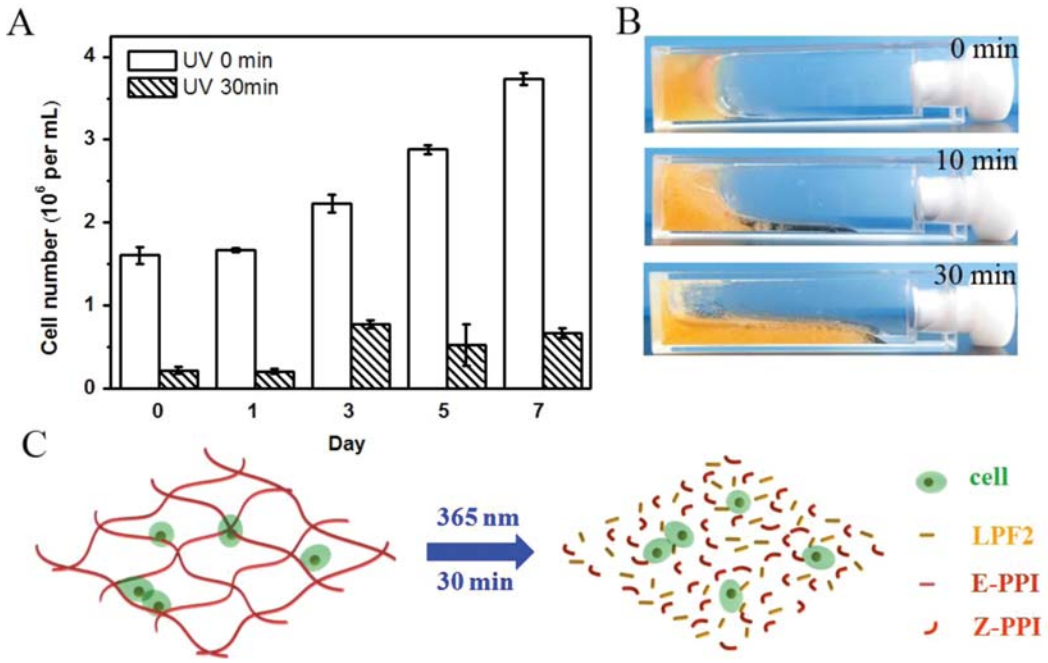

Figure 7. (A) The density of the cells encapsulated in the hydrogels before UV irradiation and the residual hydrogels after UV irradiation at different culture times. (B) Optical pictures of the LPF2-PPI hydrogel-cell construct after different times of UV exposure (an 8 W hand-held UV lamp emitting at 365 nm). (C) A schematic view of the encapsulated cells in the network of gel fibers before (left) and after (right) UV irradiation.

seeded and cultured in the hydrogel from day one to day seven (Figure 7A). The increased cell density with time suggested that cells could proliferate well in 3D hydrogels. The cell-encapsulated hydrogels were then exposed to UV light. It was observed that the gel started to collapse after 10 min of irradiation, and a complete gel-to-solution phase transition was achieved after 30 min (Figure 7B), which led to the release of the cells entrapped in the hydrogel into the bulk solution during the disruption process (Figure 7C). The changes of cell density encapsulated in hydrogels before and after UV irradiation demonstrated that not only original cultured cells were released from the hydrogels but also the proliferated cells with long culturing time could be released. It suggested the possibility to release the entrapped cells from 3D environments into aqueous solution under UV light. In comparison, negligible cell release was found in the LPF2 hydrogel before and after UV irradiation (Supporting Information, Figure S15). To further prove that the used UV power was not harmful for the cells, the viability of the released cells was evaluated by living/dead assay (Supporting Information, Figure S16b,c). These cells could spread normally and became confluent after 48 h (Supporting Information, Figure S16g), which demonstrated that the used UV light did not compromise cell viability and proliferation. Since the entire procedure did not involve any destructive factors to the cells, such as enzyme degradation, the 3D scaffold provided a facile and biologically friendly platform for controlling cell encapsulation and release in the noncontact and remote modes.

CONCLUSIONS

In summary, a multiresponsive hydrogel system was constructed through coassembly of LPF2 and PPI for the controllable cell encapsulation and release in 3D environments. UV light is used to induce the gel−sol transition and release cells entrapped in the hydrogel into aqueous solution in a noncontact mode. This study brings a novel approach to develop multistimuli-responsive hydrogels by coassembling of various responsive components for biomedical interest. It may further promote the design of advanced multistimuli-functional scaffolds for the controlled delivery of various therapeutic biological agents and bioseparation.

ASSOCIATED CONTENT

Supporting Information

Synthetic route, optical pictures, CD, FT-IR, and ^{1}H NMR spectra, XRD patterns, SEM images, and cell images. This material is available free of charge via the Internet at http://pubs.acs.org.

AUTHOR INFORMATION

Corresponding Author

*Fax: +86 2154747651. E-mail: clfeng@sjtu.edu.cn.

Notes

The authors declare no competing financial interest.

ACKNOWLEDGMENTS

This work was financially supported by the National Science Foundation of China (51173105, 51273111), the National Basic Research Program of China (973 Program 2012CB933803), and the Program for Professor of Special Appointment (Eastern Scholar) at Shanghai Institutions of Higher Learning.

REFERENCES

(1) Langer, R.; Tirrell, D. A. Designing Materials for Biology and Medicine. *Nature* **2004**, *428*, 487−492.
(2) Aida, T.; Meijer, E. W.; Stupp, S. I. Functional Supramolecular Polymers. *Science* **2012**, *335*, 813−817.

(3) Kloxin, A. M.; Kasko, A. M.; Salinas, C. N.; Anseth, K. S. Photodegradable Hydrogels for Dynamic Tuning of Physical and Chemical Properties. *Science* **2009**, *324*, 59−63.
(4) He, M.; Li, J.; Tan, S.; Wang, R.; Zhang, Y. Photodegradable Supramolecular Hydrogels with Fluorescence Turn-On Reporter for Photomodulation of Cellular Microenvironments. *J. Am. Chem. Soc.* **2013**, *135*, 18718−18721.
(5) Yang, C.; Li, D.; Liu, Z.; Hong, G.; Zhang, J.; Kong, D.; Yang, Z. Responsive Small Molecular Hydrogels Based on Adamantane-peptides for Cell Culture. *J. Phys. Chem. B* **2012**, *116*, 633−638.
(6) Mrksich, M. A Surface Chemistry Approach to Studying Cell Adhesion. *Chem. Soc. Rev.* **2000**, *29*, 267−273.
(7) Stevens, M. M.; George, J. H. Exploring and Engineering the Cell Surface Interface. *Science* **2005**, *310*, 1135−1138.
(8) Auernheimer, J.; Dahmen, C.; Hersel, U.; Bausch, A.; Kessler, H. Photoswitched Cell Adhesion on Surfaces with RGD Peptides. *J. Am. Chem. Soc.* **2005**, *127*, 16107−16110.
(9) Liu, D.; Xie, Y.; Shao, H.; Jiang, X. Using Azobenzene-Embedded Self-Assembled Monolayers to Photochemically Control Cell Adhesion Reversibly. *Angew. Chem., Int. Ed.* **2009**, *48*, 4406−4408.
(10) Yang, G.; Cao, Y.; Fan, J.; Liu, H.; Zhang, F.; Zhang, P.; Huang, C.; Jiang, L.; Wang, S. Rapid Generation of Cell Gradients by Utilizing Solely Nanotopographic Interactions on a Bio-inert Glass Surface. *Angew. Chem., Int. Ed.* **2014**, *53*, 2915−2918.
(11) Griffin, D. R.; Kasko, A. M. Photodegradable Macromers and Hydrogels for Live Cell Encapsulation and Release. *J. Am. Chem. Soc.* **2012**, *134*, 13103−13107.
(12) Yan, B.; Boyer, J.-C.; Habault, D.; Branda, N. R.; Zhao, Y. Near Infrared Light Triggered Release of Biomacromolecules from Hydrogels Loaded with Upconversion Nanoparticles. *J. Am. Chem. Soc.* **2012**, *134*, 16558−16561.
(13) Li, W.; Wang, J.; Ren, J.; Qu, X. 3D Graphene Oxide−Polymer Hydrogel: Near-Infrared Light-Triggered Active Scaffold for Reversible Cell Capture and On-Demand Release. *Adv. Mater.* **2013**, *25*, 6737−6743.
(14) Li, W.; Wang, J.; Ren, J.; Qu, X. Near-Infrared Upconversion Controls Photocaged Cell Adhesion. *J. Am. Chem. Soc.* **2014**, *136*, 2248−2251.
(15) Liu, G. F.; Zhang, D.; Feng, C. L. Control of Three-Dimensional Cell Adhesion by the Chirality of Nanofibers in Hydrogels. *Angew. Chem., Int. Ed.* **2014**, *53*, 7789−7793.
(16) Sun, Z.; Li, Z.; He, Y.; Shen, R.; Deng, L.; Yang, M.; Liang, Y.; Zhang, Y. Ferrocenoyl Phenylalanine: A New Strategy Toward Supramolecular Hydrogels with Multistimuli Responsive Properties. *J. Am. Chem. Soc.* **2013**, *135*, 13379−13386.
(17) Cravotto, G.; Cintas, P. Molecular Self-assembly and Patterning Induced by Sound Waves: The Case of Gelation. *Chem. Soc. Rev.* **2009**, *38*, 2684−2697.
(18) Cao, W.; Zhang, X.; Miao, X.; Yang, Z.; Xu, H. γ-Ray-Responsive Supramolecular Hydrogel Based on a Diselenide-Containing Polymer and a Peptide. *Angew. Chem., Int. Ed.* **2013**, *52*, 6233−6237.
(19) Yan, X.; Xu, D.; Chi, X.; Chen, J.; Dong, S.; Ding, X.; Yu, Y.; Huang, F. A Multiresponsive, Shape-Persistent, and Elastic Supramolecular Polymer Network Gel Constructed by Orthogonal Self-Assembly. *Adv. Mater.* **2012**, *24*, 362−369.
(20) Qi, Z.; Malo de Molina, P.; Jiang, W.; Wang, Q.; Nowosinski, K.; Schulz, A.; Gradzielski, M.; Schalley, C. A. Systems Chemistry: Logic Gates Based on the Stimuli-Responsive Gel-Sol Transition of a Crown Ether-Functionalized Bis(urea) Gelator. *Chem. Sci.* **2012**, *3*, 2073−2082.
(21) Liu, J.; He, P.; Yan, J.; Fang, X.; Peng, J.; Liu, K.; Fang, Y. An Organometallic Super-Gelator with Multiple-Stimulus Responsive Properties. *Adv. Mater.* **2008**, *20*, 2508−2511.
(22) Liu, Z.-X.; Feng, Y.; Yan, Z.-C.; He, Y.-M.; Liu, C.-Y.; Fan, Q.-H. Multistimuli Responsive Dendritic Organogels Based on Azobenzene-Containing Poly(aryl ether) Dendron. *Chem. Mater.* **2012**, *24*, 3751−3757.
(23) Duan, P.; Li, Y.; Li, L.; Deng, J.; Liu, M. Multiresponsive Chiroptical Switch of an Azobenzene-Containing Lipid: Solvent, Temperature, and Photoregulated Supramolecular Chirality. *J. Phys. Chem. B* **2011**, *115*, 3322−3329.
(24) Buerkle, L. E.; Rowan, S. J. Supramolecular Gels Formed from Multi-Component Low Molecular Weight Species. *Chem. Soc. Rev.* **2012**, *41*, 6089−6102.
(25) Smith, A. M.; Williams, R. J.; Tang, C.; Coppo, P.; Collins, R. F.; Turner, M. L.; Saiani, A.; Ulijn, R. V. Fmoc-Diphenylalanine Self Assembles to a Hydrogel via a Novel Architecture Based on $\pi-\pi$ Interlocked β-Sheets. *Adv. Mater.* **2008**, *20*, 37−41.
(26) Yamaguchi, H.; Kobayashi, Y.; Kobayashi, R.; Takashima, Y.; Hashidzume, A.; Harada, A. Photoswitchable Gel Assembly Based on Molecular Recognition. *Nat. Commun.* **2012**, *3*, 603−608.
(27) Khetan, S.; Guvendiren, M.; Legant, W. R.; Cohen, D. M.; Chen, C. S.; Burdick, J. A. Degradation-Mediated Cellular Traction Directs Stem Cell Fate in Covalently Crosslinked Three-Dimensional Hydrogels. *Nat. Mater.* **2013**, *12*, 458−465.
(28) Ren, T.; Li, L.; Cai, X.; Dong, H.; Liu, S.; Li, Y. Engineered Polyethylenimine/Graphene Oxide Nanocomposite for Nuclear Localized Gene Delivery. *Polym. Chem.* **2012**, *3*, 2561−2569.
(29) van Bommel, K. J. C.; van der Pol, C.; Muizebelt, I.; Friggeri, A.; Heeres, A.; Meetsma, A.; Feringa, B. L.; van Esch, J. Responsive Cyclohexane-Based Low-Molecular-Weight Hydrogelators with Modular Architecture. *Angew. Chem., Int. Ed.* **2004**, *43*, 1663−1667.
(30) Fang, W.; Sun, Z.; Tu, T.; Novel Supramolecular, Thixotropic Metallohydrogels Consisting of Rare Metal−Organic Nanoparticles: Synthesis, Characterization, and Mechanism of Aggregation. *J. Phys. Chem. C* **2013**, *117*, 25185−25194.
(31) Zhang, S.; Gelain, F.; Zhao, X. Designer Self-assembling Peptide Nanofiber Scaffolds for 3D Tissue Cell Cultures. *Semin. Cancer Biol.* **2005**, *15*, 413−420.
(32) Sun, W.; Puzas, J. E.; Sheu, T. J.; Liu, X.; Fauchet, P. M. Nano- to Microscale Porous Silicon as a Cell Interface for Bone-Tissue Engineering. *Adv. Mater.* **2007**, *19*, 921−924.